SLAC−PUB−10850

Longitudinal phase space tomography at the SLAC Gun Test Facility and the BNL DUV-FEL

H. Loos[a*], P.R. Bolton[b], J.E. Clendenin[b], D.H. Dowell[b], S.M. Gierman[b], C.G. Limborg[b], J.F. Schmerge[b], T.V. Shaftan[a], B. Sheehy[a]

[a]National Synchrotron Light Source, Brookhaven National Laboratory, Upton, NY 11973, USA

[b]Stanford Linear Accelerator Center, Menlo Park, CA 94025, USA

The Gun Test Facility (GTF) and the accelerator at the DUV-FEL facility are operated as sources for high brightness electron beams; the first for the Linac Coherent Light Source project and the latter driving an FEL using High Gain Harmonic Generation (HGHG) in the UV. For both accelerators, projections of the longitudinal phase space on the energy coordinate were obtained by varying the phase of an accelerating structure after the gun and measured with a downstream spectrometer dipole. Using an algebraic reconstruction technique (ART), the longitudinal phase space at the entrance to the varied accelerating structure could be reconstructed over a large range of charge from 15 pC to 600 pC.

Key words: Relativistic electron beams, Beam dynamics, Tomography
PACS: 41.75.Ht, 29.27.Bd, 42.30.Wb

1. Introduction

Accelerators for existing and future high brightness electron beam sources require high peak current usually achieved by magnetic bunch compression. A measurement of the longitudinal electron phase space can be useful in understanding and optimizing both injector dynamics and bunch compression. Tomographic methods have been employed to reconstruct the phase space in recent years [1–3] using measurements of energy spectra with varying longitudinal chirp and dispersion. The technique provides a model independent determination of the phase space as well as a measurement of the slice energy spread of the bunch.

The experiments reported in this paper were done at the Gun Test Facility (GTF) at SLAC and the DUV-FEL at BNL. The GTF accelerator [4] consists of a BNL/SLAC/UCLA 1.6 cell gun with a Nd:Glass drive laser (2 ps FWHM), a 25 MeV s-band accelerating structure, and a dipole energy spectrometer about 3 keV resolution, where the energy spectra were taken while varying the linac phase. The DUV-FEL accelerator [5] shares the gun and accelerating structure with GTF, but the cathode drive laser is Ti:Sapphire based and there are three additional accelerating structures for up to 200 MeV beam energy and a chicane bunch compressor behind the second linac tank.

2. Reconstruction Technique

Various methods have been developed in the past decades in the field of computerized tomographic imaging to retrieve the original two dimensional distribution from a set of measured projections of this distribution. The Simultaneous Algebraic Reconstruction Technique (SART) [6] uses an iterative method to solve the set of linear equations coupling the image and its projections. If the original image is described as discrete pixels g_l, then the ith projection histogram $p_{i,j}$ can be calculated as a sum of the image along the rays of the given projection with the weight

*loos@bnl.gov

Work supported in part by the Department of Energy Contract DE−AC02−76SF00515

Presented at 25th International Free Electron Laser Conference (FEL 2003) and 10th FEL User Workshop, 9/8/2003 - 9/12/2003, Tsukuba, Ibaraki, Japan

coefficients $a_{i,jl}$ according to

$$p_{i,j} = \sum_{jl} a_{i,jl} g_l. \quad (1)$$

Starting from an image $g_q^{(0)}$ as initial guess an iteration step

$$g_q^{(k+1)} = g_q^{(k)} + \sum_j \frac{a_{i,jq}\left(p_{i,j} - \sum_l a_{i,jl}\, g_l^{(k)}\right)}{\sum_{nl} a_{i,nl}^2} \quad (2)$$

uses one projection p_i after the other until all are utilized once. This procedure is then iterated itself until convergence is reached, which usually occurs within a couple of iterations.

In order to apply this method to the reconstruction of the longitudinal electron phase space distribution $g(\tau, \delta)$, with τ as time coordinate and δ the energy deviation of a particle from the beam centroid energy, the phase space is segmented into discrete bins g_l with size $\Delta\tau$ and $\Delta\delta$. Accelerating the electron beam with initial energy E_0 in a linac section with energy gain V results in a beam energy of $E = E_0 + V\cos(\phi)$ and an energy deviation of $\delta' = \delta + k\tau$ with the chirp $k = -V\sin(\phi)$. A set of energy spectra is then obtained at different accelerating phases ϕ_i with the spectra as histograms $p_{i,j}$ having the same bin size $\Delta\delta$ as the phase space. The weight coefficients $a_{i,jl}$ for the projections are determined by tracing each phase space pixel according to the applied chirp onto the energy axis. Using the coefficient matrix and measured energy spectra, the phase space can be reconstructed with Eq. 2.

Since this implementation of the tomographic reconstruction only uses an off-crest acceleration and no preceding dispersive element, the set of projections do not include a full 90° rotation of the phase space, i.e., a projection of the time coordinate onto the energy axis. Therefore, the temporal resolution of the reconstructed phase space will be limited due to the maximum chirp $k_{\max}$ applied to the beam. In this case, temporal structures converted into an energy distribution are folded with the slice energy spread $\sigma_{\delta,0}$. Considering both a correlated energy modulation and a temporal density modulation the highest frequency that can be resolved is given by

$$f_{\mathrm{res}} = k_{\max}/(2\pi\sigma_{\delta,0}). \quad (3)$$

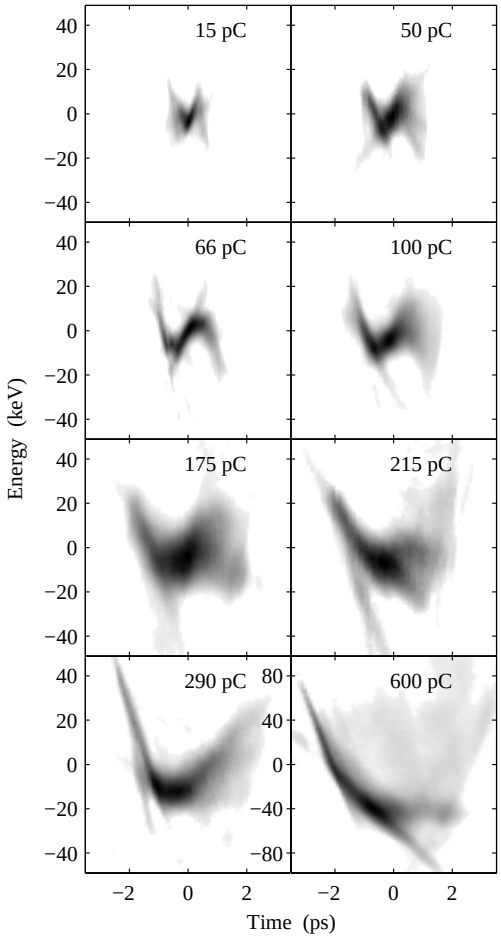

Figure 1. Reconstructed phase space distribution for GTF at linac entrance.

3. GTF Measurements

The analysis is based on energy spectra measurements presented in [4]. A fit to the beam energy and energy spread determines the accelerating voltage of the linac structure, the phase difference between maximum energy and minimum spread, and parameters of the longitudinal phase space ellipse at the linac entrance. To minimize the rectangular phase space region of the reconstruction, the chirp k is calculated in respect to

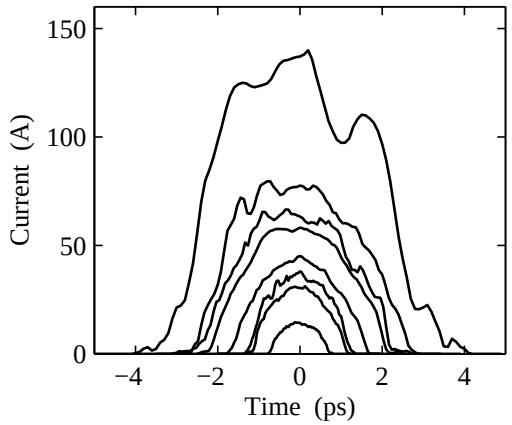

Figure 2. Temporal projection of the reconstructions as shown in Fig. 1. The bunch charge for the different curves with increasing peak current are 15, 50, 66, 100, 175, 215, 290, and 600 pC, respectively.

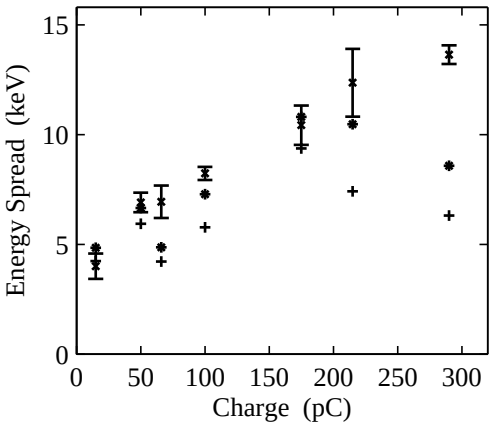

Figure 3. Slice energy spread from reconstructions as shown in Fig. 1. The "x" symbols are the projected, the "∗" symbols are the averaged slice, and the "+" symbols represent the slice energy spread at maximum peak current.

the phase with minimum spread, thus ignoring the linear chirp of the beam entering the linac.

The phase range of usually 60° corresponds to a maximum chirp of $k_{\max} = 220\,\mathrm{keV/ps}$. A simulation of the experiment with a time and energy modulated phase space was performed to determine the time and energy resolution achievable for the measured energy spectra. The estimate of Eq. 3 was confirmed, giving a resolution of 150 to 300 fs for a slice energy spread of 5 to 10 keV.

The reconstructed phase space distributions are shown in Fig. 1. A 7% intensity cut was applied to remove residual artifacts from linac phase and amplitude drifts during the measurement. The bunch current profile obtained from the reconstructions is shown in Fig. 2. Compared with the cathode laser duration of 2 ps (FWHM) the electron beam is compressed below 100 pC and elongated above. The profiles show some structure which can be attributed to remaining artifacts. The analysis of the energy spread is shown in Fig. 3. The projected energy spread is taken from the longitudinal beam ellipses, whereas the slice data are obtained by a gaussian fit to the energy profile of each time slice. The average slice energy spread is growing almost as fast with charge as the projected due to increasing spread in the bunch tails. However, the slice energy spread taken at the peak of the current distribution exhibits a significant smaller growth with increasing charge.

4. DUV-FEL Measurement

The measurement at the DUV-FEL accelerator was done by varying the phase of the second accelerating structure while the chicane and tanks 3 and 4 were not used. The maximum chirp was 200 keV/ps, resulting in a time resolution of 250 ps for 8 keV energy spread. Figure 4 shows the reconstructed phase space at the entrance of tank 2 with bunch charge of 200 pC and energy of 38 MeV. Due to a three times longer laser pulse of 2.35 ps compared to GTF, the electron bunch is still ballistically compressed to 1.35 ps. The corresponding drive laser time profile in Fig. 5 exhibits three main substructures as a consequence of the large bandwidth of the Ti:Sa oscillator.

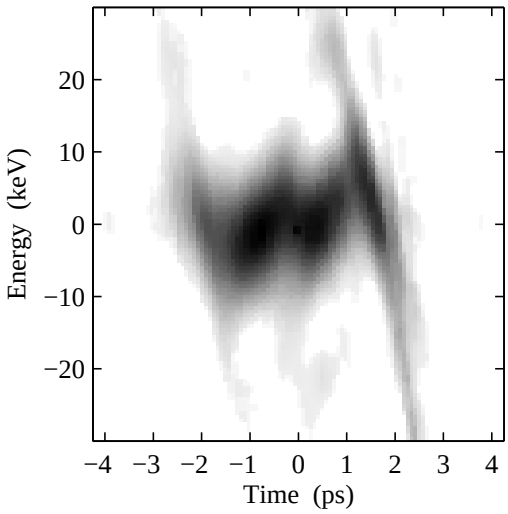

Figure 4. Reconstructed longitudinal phase space distribution of the DUV-FEL accelerator at the entrance of the second linac tank for a charge of 200 pC.

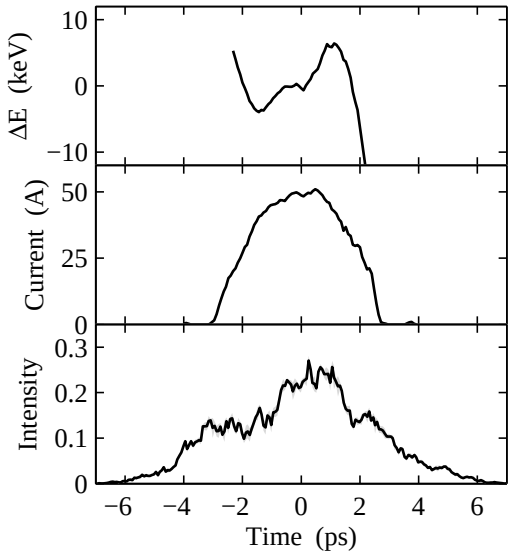

Figure 5. Temporal distributions corresponding to the reconstruction as shown in Fig. 4. The bottom part shows the measured cathode drive laser distribution, the middle part the reconstructed electron beam current, and to top part the energy – time correlation.

The structures are not visible in the time distribution of the electron beam, however, they can be recognized in the phase space where they appear as energy time correlation. This can be attributed to longitudinal space charge (LSC) effects [7].

5. Conclusion

An algebraic reconstruction technique was used to reconstruct the longitudinal electron phase space at GTF and DUV-FEL for different bunch charges. The slice energy spread can be significantly smaller than the projected due to nonlinear energy time correlations. Simulations of the injector dynamics to better understand these observations are in progress for both facilities. The implementation of the technique to the compressed bunch at DUV-FEL is planned for the future.

This work was supported by DOE contracts DE-AC03-76SF00515 and DE-AC02-98CH10886.

REFERENCES

1. E.R. Crosson et al., Nucl. Instrum. Meth. A 375 (1996) 87
2. M. Hüning, Investigations of the longitudinal charge distribution in very short electron bunches, Proceedings of DIPAC 2001, ESRF, Grenoble
3. S. Kashiwagi et al., Proceedings of the XX International Linac Conference, Monterey, CA, 2000, p. 149
4. D.H. Dowell et al., Nucl. Instrum. Meth. A 507 (2003) 331
5. W.S. Graves et al., Proceedings of the 19th Particle Accelerator Conference, Chicago, IL, June 2001, p. 2224
6. A.C. Kak, M. Slaney, Principles of Computerized Tomographic Imaging, IEEE Press, 1979
7. T. Shaftan et al., these proceedings, TU-P-66